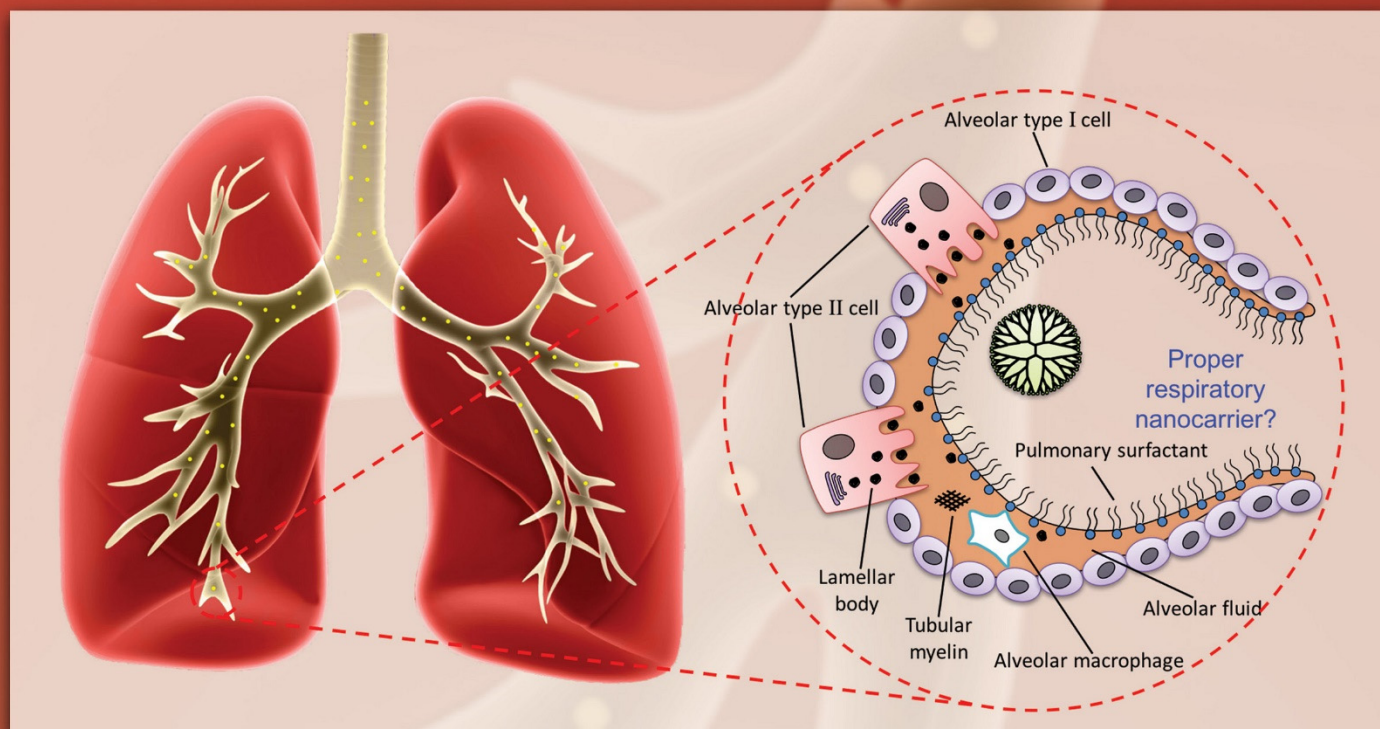


LANGMUIR

The ACS journal of fundamental interface science



Poly(amidoamine) Dendrimer as a Respiratory Nanocarrier: Insights from Experiments and Molecular Dynamics Simulations

Fujia Tian,[†] Xubo Lin,^{*,†,‡,§,||} Russell P. Valle,^{||} Yi Y. Zuo,^{*,||} and Ning Gu^{*,§,||}

[†]Beijing Advanced Innovation Center for Biomedical Engineering, Beihang University, Beijing 100083, China

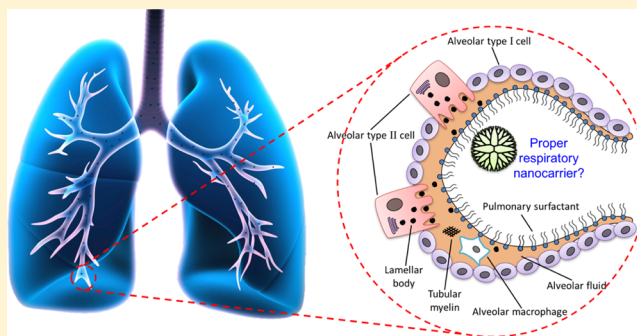
[‡]Key Laboratory of Ministry of Education for Biomechanics and Mechanobiology, School of Biological Science and Medical Engineering, Beihang University, Beijing 100083, China

[§]State Key Laboratory of Bioelectronics and Jiangsu Key Laboratory for Biomaterials and Devices, School of Biological Science & Medical Engineering, Southeast University, Nanjing 210096, China

^{||}Department of Mechanical Engineering, University of Hawaii at Manoa, Honolulu, Hawaii 96822, United States

S Supporting Information

ABSTRACT: Pulmonary drug delivery is superior to the systemic administration in treating lung diseases. An optimal respiratory nanocarrier should be able to efficiently and safely cross the pulmonary surfactant film, which serves as the first biological barrier for respiratory delivery and plays paramount roles in maintaining the proper mechanics of breathing. In this work, we focused on the interactions between poly(amidoamine) (PAMAM) dendrimers and a model pulmonary surfactant. With combined Langmuir monolayer experiments and coarse-grained molecular dynamics simulations, we studied the effect of environmental temperature, size, and surface property of PAMAM dendrimers (G3-OH, G3-NH₂, G5-OH, and G5-NH₂) on the dipalmitoylphosphatidylcholine (DPPC) monolayer. Our simulations indicated that the environmental temperature could significantly affect the influence of PAMAM dendrimers on the DPPC monolayer. Therefore, results obtained at room temperature cannot be directly applied to elucidate interactions at body temperature. Simulations at body temperature found that all tested PAMAM dendrimers can easily penetrate the lipid monolayer during the monolayer expansion process (mimicking “inhalation”), and the cationic PAMAM dendrimers (–NH₂) show promising penetration ability during the monolayer compression process (mimicking “expiration”). Larger PAMAM dendrimers (G5) adsorbed onto the lipid monolayer tend to induce structural collapse and inhibit normal phase transitions of the lipid monolayer. These adverse effects could be mitigated in the subsequent expansion–compression cycle. These findings suggest that the PAMAM dendrimer may be used as a potential respiratory drug nanocarrier.



INTRODUCTION

In the past decades, nanoscale drug carriers have been widely developed. However, delivery efficiencies for cancer nanomedicines are still low.^{1–3} Systemic delivery of drugs to the targeted organs is not easy. Hence, more attention has been paid to respiratory drug delivery to treat lung diseases.^{4–6} Dendrimers, as one kind of popular nanoscale drug carriers, are a class of polymeric nanoparticles with regularly successive building blocks initiating from a central core molecule.^{7–10} The branched repeating building units are described by generation (Figure 1a).¹¹ Dendrimers have been extensively investigated because of their unique properties and architectures, such as deformable conformation, well-defined size, easy surface modification, favorable water solubility, controllable cytotoxicity, and polydispersity.^{12,13} However, it is still unknown whether dendrimers are suitable for delivering drugs via the respiratory pathway. In this work, we focus on

one of the most representative dendrimers: poly(amidoamine) (PAMAM) dendrimers.^{14,15}

To be an efficient and safe nanoscale respiratory drug carrier, PAMAM dendrimers need to penetrate the biological barriers in the lungs without significantly affecting their structures and functions. The first biological barrier for respiratory drug delivery is the pulmonary surfactant (PS). It is a film mainly containing lipids and surfactant-associated proteins. The PS film adsorbs onto the air–water interface of the alveoli. It plays a vital role in reducing the surface tension of the lungs to maintain the proper mechanics and to avoid alveolar collapse.^{16,17} Dipalmitoylphosphatidylcholine (DPPC) is the most abundant single component in natural PS. Hence, the DPPC monolayer self-assembled at the air–water surface has

Received: February 12, 2019

Revised: March 15, 2019

Published: March 19, 2019

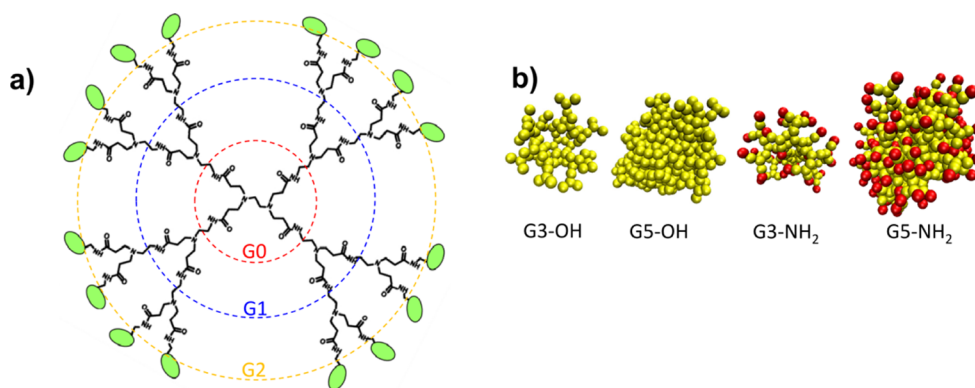


Figure 1. (a) Schematic of the repeated branched structures for the PAMAM dendrimer using the generation 2 (G2) PAMAM dendrimer as an example. Surface terminals are shown in green ellipse. (b) CG snapshots of all PAMAM dendrimers studied in this work. Charged surface terminals are colored in red, while others in yellow.

been widely used as a PS model to understand the biophysical role of PS films.^{18–21} The DPPC monolayer experiences phase transitions between the liquid-expanded (LE) and the liquid-condensed (LC) phases during compression and expansion processes.^{16,22–25} Research shows that PAMAM dendrimers can disrupt lipid bilayers.^{26–29} However, it is still unclear whether inhaled PAMAM dendrimers have adverse impacts on the function of PS films. Hence, we focused on interactions between PAMAM dendrimers, as a model drug nanocarrier, and the DPPC monolayer, as a model PS film.

Both in vitro experiments^{30–32} and molecular dynamics (MD) simulations^{18,26,33–37} have been widely used to study interactions between nanoparticles and the PS film. Many efforts have been made to reveal the effects of rigid inorganic nanoparticles on the PS film.^{26,34,35,38,39} In the current work, we focused on interactions between the flexible PAMAM dendrimer and DPPC monolayers using MD simulations and Langmuir monolayer experiments. Our results indicated that large PAMAM dendrimers induce membrane protrusions and inhibit normal phase transitions of the interfacial lipids during the monolayer compression process. These adverse effects of PAMAM dendrimers on the DPPC monolayer could be greatly reduced in the subsequent monolayer expansion process. All PAMAM dendrimers could cross the DPPC monolayer rapidly during the expansion process and small charged PAMAM dendrimers successfully permeated into the aqueous phase during the compression process. In other words, PAMAM dendrimers can easily pass through the model PS without significantly disrupting its structure and functions during the compression–expansion cycles. In addition, we found that the environmental temperature could dramatically change the responses of the DPPC monolayer to PAMAM dendrimers, which indicated that results at room temperature could not be simply and directly used to elucidate the interaction mechanism at body temperature.

MATERIALS AND METHODS

Materials. Hydroxyl (–OH)- or amino (–NH₂)-modified G3 and G5 PAMAM dendrimers were purchased from Dendritech Inc. (Midland, MI). DPPC was purchased from Avanti Polar Lipids (Alabaster, AL) and used without further purification. All solvents used were high-performance liquid chromatography grade. The water used was Milli-Q ultrapure water (Millipore, Billerica, MA), which has a resistivity higher than 18 MΩ·cm at room temperature (20 ± 1 °C).

Langmuir Monolayer Experiments. Compression isotherms of the DPPC monolayer were obtained with a Langmuir–Blodgett (LB)

trough (KSV Nima, Coventry, UK) at room temperature (20 ± 1 °C). The DPPC monolayer was prepared by uniformly spreading tiny droplets of 1 mg/mL DPPC dissolved in chloroform throughout the air–water surface using a 10 μL microsyringe. The system was left undisturbed for 10 min to allow evaporation of the solvent. Subsequently, PAMAM dendrimers were spread atop the DPPC monolayer at a 1:1024 molar ratio and left for 10 min to allow equilibrium. The film was compressed at a speed of 20 cm²/min and the surface pressure–area (π -A) isotherm was recorded. Generally, the whole compression process takes about 8 min.

For atomic force microscopy (AFM) imaging, the DPPC monolayer at the air–water surface was transferred to a freshly cleaved mica surface using the LB technique. Monolayers under controlled surface pressures of 5 mN/m, that is, in the middle of the phase transition plateau, were deposited onto the mica surface by elevating the previously submerged mica vertically through the air–water surface at a rate of 1 mm/min. Deposited monolayers were scanned by AFM within 2 h of deposition. Topographical images were obtained using an Innova AFM (Bruker, Santa Barbara, CA). Each sample was characterized at multiple locations with various scan areas to ensure the detection of representative structures. Both the contact mode and tapping mode were used. The different scan modes gave equivalent results. A silicon nitride cantilever with a spring constant of 0.12 N/m and a nominal tip radius of 2 nm was used in the contact mode, and a silicon probe with a resonance frequency of 300 kHz and a spring constant of 40 N/m was used in the tapping mode. Analysis of the AFM images was performed using NanoScope software (version 7.30).

MD Simulations. The coarse-grained (CG) MD simulation of interactions between PAMAM dendrimers and DPPC monolayers was employed using GROMACS simulation package⁴⁰ with the MARTINI 2.0 force field developed by Marrink et al.^{41,42} In general, MARTINI model maps four heavy atoms into one interaction site. For the aromatic group, it adopts the 2 or 3 to 1 mapping rule. Standard parameters for DPPC, water, and salt ions (Na⁺, Cl[–]) were used. As for the PAMAM dendrimer, MARTINI-compatible parameters developed by Lee and Larson,^{43,44} which well reproduced the dynamical behaviors of PAMAM dendrimers interacting with the lipid membrane, were used in this work. PAMAM dendrimers of two different sizes (generation 3, G3; generation 5, G5) and two different surface functional groups (–OH, neutral; –NH₂, positively charged) were studied (Figure 1b). As a result, G3 and G5 PAMAM dendrimers have 122 and 506 CG beads in total, 32 and 128 surface CG beads correspondingly. A bimonolayer system consisting of 2048 DPPC molecules and 58 240 CG water molecules as well as 150 mM salt ions was used to study the interactions between PAMAM dendrimers and the DPPC monolayer at the air–water surface. The air phase was represented by vacuum, which was widely used in current state-of-art MD simulations and able to reproduce the key dynamics of the lipid monolayer at the air–water interface in the

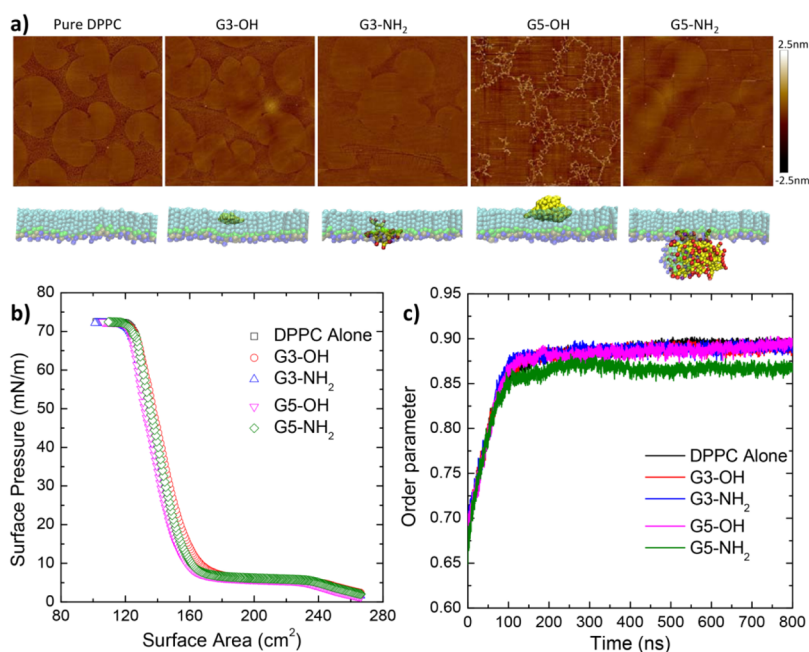


Figure 2. Comparison of Langmuir monolayer experiments and MD simulations of PAMAM dendrimer–DPPC interactions at room temperature ($T = 295$ K). (a) AFM images of the DPPC monolayer without and with various PAMAM dendrimers (upper panel) and MD simulations (lower panel, side-view). (b) Surface pressure–area isotherms of the DPPC monolayer without and with various PAMAM dendrimers obtained with the Langmuir monolayer experiments. (c) Time evolution of interfacial lipid chain order parameters obtained with MD simulations.

Langmuir experiments. The average area per lipid for the starting configurations of the compression and expansion simulations were set as 0.563 nm^2 (fully LE phase) and 0.477 nm^2 (fully LC phase), respectively.^{35,38} Inhaled PAMAM dendrimers were modeled by placing them in the air side near the tails of DPPC molecules. For all simulations, periodic boundary conditions were applied in all three dimensions. A standard 1.2 nm cutoff was applied for van der Waals interactions, and L-J potential was shifted to zero smoothly from 0.9 to 1.2 nm to avoid cutoff noise. For Coulombic potential, a 1.2 nm cutoff was used for short-range electrostatic interactions with shifting to zero from 0 to 1.2 nm smoothly. The default value (15) of the force field was used for the relative dielectric constant.⁴¹ Lipids, water, ions and PAMAM dendrimers were coupled to 310 or 295 K using the Berendsen thermostat⁴⁵ with a relaxation time $\tau = 1 \text{ ps}$. The lateral pressure was kept at 1 bar by semi-isotropic Berendsen pressure coupling⁴⁵ (coupling constant is 4 ps . Compressibility in the lateral direction is $5 \times 10^{-5} \text{ bar}^{-1}$ and is zero in the normal direction). For each system, the compression–expansion simulation was run for 800 ns with a time step of 20 fs . The neighbor list of nonbonded interactions was updated every 10 steps. It is worth mentioning that it is impossible to reach the time scale of 8 min (mentioned above) in coarse-grained molecular dynamics (CGMD) simulations. Hence, we use the popular bilayer system with the lateral pressure of 1 bar to achieve affordable time scale (800 ns) in our simulations, which well reproduced the basic changes of the structure and normal phase transition of interfacial DPPC molecules during the compression–expansion processes.^{34,35,38}

Lipid Chain Order Parameter. Lipid chain order parameter (S_z) was calculated using the formula

$$S_{z,n} = \left\langle \frac{1}{2} (3 \cos^2 \theta_n - 1) \right\rangle$$

where θ_n is the angle between the vector connecting the $n - 1$ and $n + 1$ sites of the tail and bilayer normal z . S_z is averaged over the two lipid chains and the entire bilayer to compare lipid chain order parameters among different systems.

RESULTS AND DISCUSSION

Langmuir Monolayer Experiments and MD Simulations Show Consistent Results at Room Temperature.

In order to validate our MARTINI CG model, we studied the interactions between PAMAM dendrimers (Figure 1b) and DPPC monolayers at the air–water interface using Langmuir monolayer experiments at room temperature ($T = 295 \text{ K}$). Figure 2a shows AFM images and computational snapshots for the final states of the DPPC monolayer under compressions. G3-OH and G5-OH PAMAM dendrimers failed to cross the DPPC monolayer during the compression process (Figure S1). For the G3-OH PAMAM dendrimer, the lipid monolayer shows no differences compared to the pure DPPC monolayer. This is most likely because G3-OH is very small and easy to embed itself into the hydrophobic region of the DPPC monolayer. The G5-OH PAMAM dendrimer is much larger than G3-OH, and hence stands on the terminals of the hydrophobic lipid tails, thus forming a network standing out of the DPPC monolayer. Both G3-NH₂ and G5-NH₂ PAMAM dendrimers penetrate the aqueous phase (Figure S1). Thus, there are no obvious differences between these two systems and the pure DPPC monolayer as observed by AFM. In general, our MD simulations are in good agreement with the AFM observations.

The monolayer experiments show that PAMAM dendrimers possess little effects on the surface pressure–area isotherm profiles of the DPPC monolayer (Figure 2b). The phase transition plateaus¹⁶ of interfacial lipid acyl chains overlap intensely well (Figure 2b). It means that no PAMAM dendrimers studied here significantly inhibit the normal phase transition of the DPPC monolayer. This is consistent with our CGMD simulations at room temperature ($T = 295 \text{ K}$), which is indicative that PAMAM dendrimers do not affect the time evolution of interfacial lipid chain order parameters during the compression process (Figures 2c and S2). However,

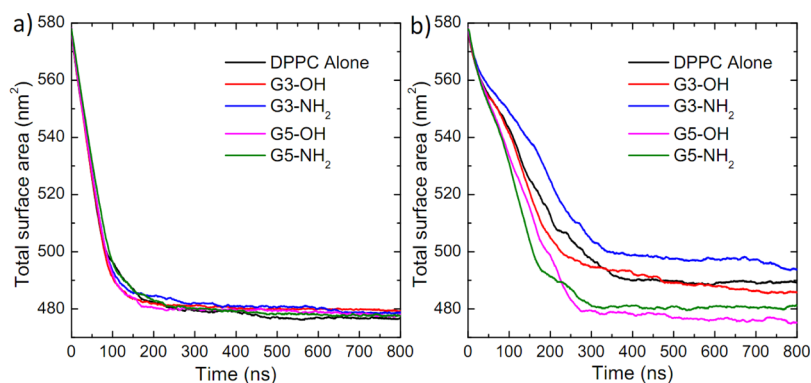


Figure 3. Time evolution of the total interfacial surface in the interactions of PAMAM dendrimers and the DPPC monolayer at the air–water interface during the compression process (a) at room temperature ($T = 295$ K) and (b) body temperature ($T = 310$ K).

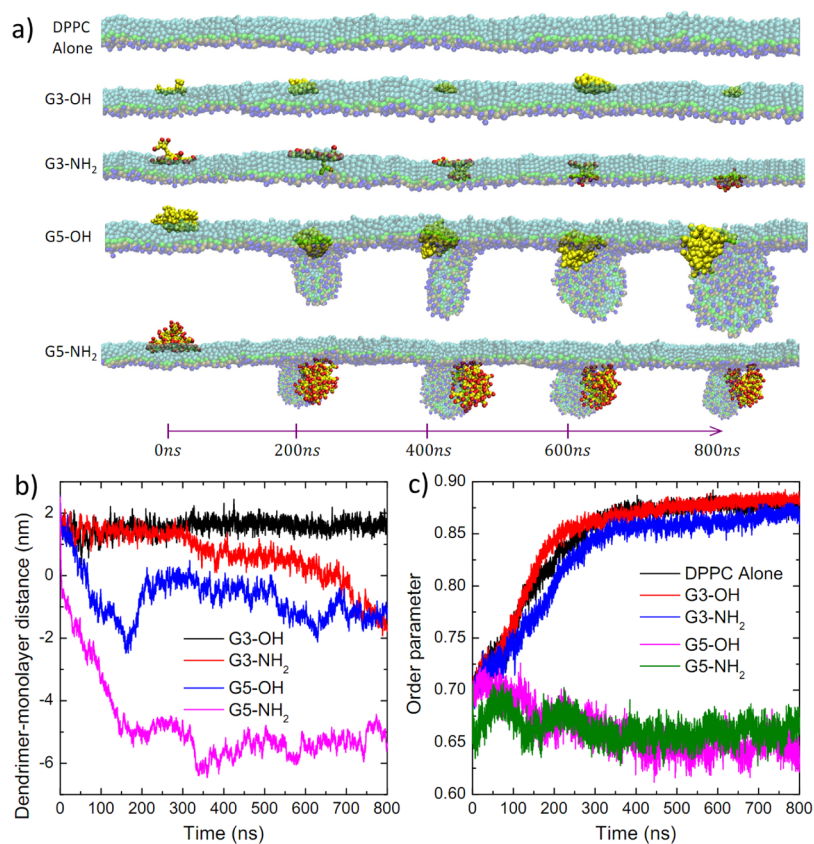


Figure 4. (a) Time-varied changes of system conformations, (b) dendrimer-monolayer distances, and (c) interfacial lipid chain order parameters in the interactions between PAMAM dendrimers and the DPPC monolayer at the air–water interface during the compression process at body temperature ($T = 310$ K).

our previous CGMD simulations at body temperature demonstrated that PAMAM dendrimers significantly disturb the phase transitions of DPPC monolayers.³⁴ Therefore, comparison of these results indicates critical roles of the environmental temperature in the interactions of PAMAM dendrimers with the model PS membrane at the air–water interface.

To further confirm the importance of environmental temperature, we did a direct comparison between CGMD simulations during the compression process at both room temperature and body temperature. As shown in Figure 3, PAMAM dendrimers have little effects on the time evolution of total lateral surface area at room temperature (Figure 3a).

Combined the results mentioned above, we can conclude that PAMAM dendrimers do not disturb the dynamics of interfacial lipids during the compression process at room temperature. However, when the environmental temperature is increased to body temperature, time evolution of the total lateral surface area for the pure DPPC monolayer system is dramatically changed (Figure 3b). The responses of the DPPC monolayer to different PAMAM dendrimers became much more sensitive at elevated temperature. It means that results at room temperature cannot be directly used to elucidate the interaction mechanism between PAMAM dendrimers and the lipid monolayer at body temperature.

Larger PAMAM Dendrimer Shows Adverse Effects on the DPPC Monolayer during the Compression Process at Body Temperature.

Small hydrophilic nanocarriers were reported to cross the lipid monolayer easily with little side effects.^{35,38} As mentioned above, the PAMAM dendrimer is hydrophilic, flexible, and has easy-modified surface terminals and internal voids, which makes it probably suitable for respiratory drug nanocarrier. Also, we considered these PAMAM dendrimers with two different sizes (G3, G5) and two different surface functional groups ($-OH$, neutral; $-NH_2$, positively charged) for cases of body temperature (Figure 1b). PAMAM dendrimers (G3-OH, G3-NH₂, G5-OH, and G5-NH₂) were placed in the “gas” phase near the DPPC monolayer to model inhaled nanocarriers. The environmental temperature was set to body temperature (310 K). Figure 4a shows the structural changes of DPPC monolayers at the air–water interface with/without the interactions of PAMAM dendrimers during the compression process. Generally, small-size PAMAM dendrimers (G3) have little effects on the structure of the DPPC monolayer, while large-size PAMAM dendrimers (G5) tend to induce the membrane protrusion toward the aqueous phase (“fold” structure¹⁶). In the case of membrane protrusions, G5 PAMAM dendrimers directly interact with the “fold” structure rather than interfacial DPPC molecules. Charged surface terminals ($-NH_2$) can significantly enhance the membrane penetration ability of PAMAM dendrimers (Figure 4b). Within our simulation time, G3-NH₂ and G5-NH₂ completely crossed the DPPC monolayer and stayed at the lipid head-group region. The preferred interaction of PAMAM dendrimers with the lipid head-group in our monolayer system is mainly determined by the electrostatic interactions, which is consistent with that in the bilayer system.^{11,46} In addition, unlike the rigid nanoparticles,^{26,35} PAMAM dendrimers can minimize the resistance force by dynamically adjusting an optimal shape during the penetration process. In other words, the flexibility of PAMAM dendrimers also contributes to its potent penetration ability. We further monitored the time evolution of interfacial lipid acyl chain order parameters. As shown in Figure 4c, G3 PAMAM dendrimers show little effects on the order parameter evolution trend, while G5 PAMAM dendrimers can suppress the increase of interfacial lipid acyl chain order parameters. This is consistent with the size effects of PAMAM dendrimers on the structural disruption of DPPC monolayers (Figure 4a). Moreover, we further used the two-dimensional (2D) phase map to describe the detailed information for the normal phase-transition inhibition of the interfacial lipid acyl chains. As shown in Figure 5, each 2D phase map contains both the position of each interfacial lipid and its corresponding chain-order parameter. From the whole time evolution process of the 2D phase maps, the normal phase transition (LE phase \rightarrow LE–LC coexisting phase \rightarrow LC phase) inhibition of the interfacial lipid acyl chains during the compression process is confirmed. On the one hand, combining the structural disruptions (Figure 4a) and phase behaviors (Figures 4c and 5) of DPPC monolayers, we can conclude that PAMAM dendrimer-induced membrane protrusions (“fold” structure) bring about the inhibition of this normal phase transition. On the other hand, for cases of large-size PAMAM dendrimers (G5), the interfacial DPPC molecules are still keeping the LE phase rather than the LC phase at the end of the compression process, which will dramatically change the mechanics and matter-exchange ability of the DPPC monolayer at the air–

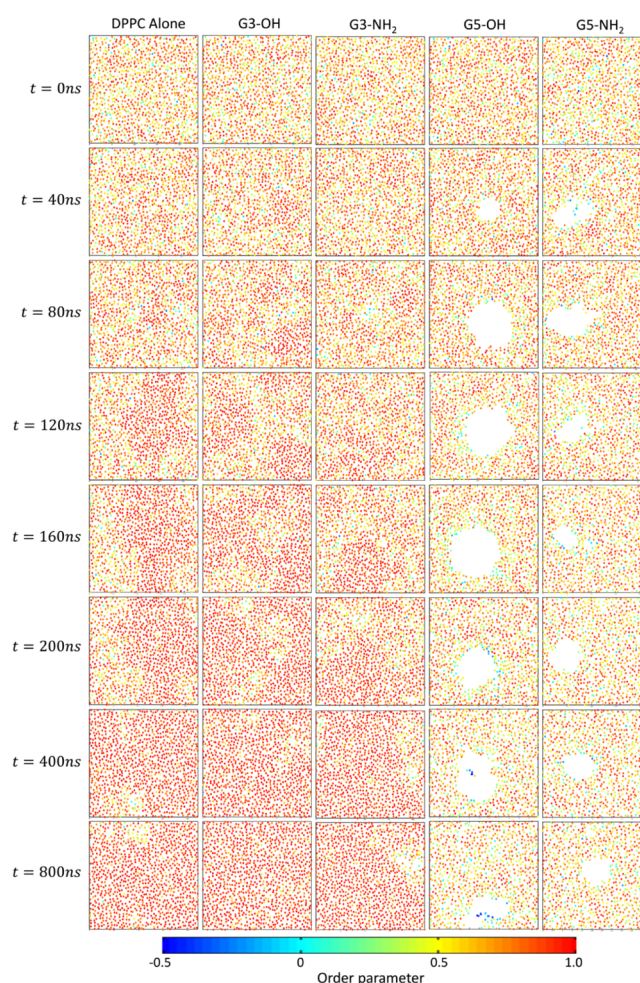


Figure 5. Phase behaviors of the interfacial DPPC molecules in the interactions of PAMAM dendrimers with the DPPC monolayer at the air–water interface during the compression process at body temperature ($T = 310$ K). Each point represents one DPPC molecule, and its color shows the averaged chain order parameters.

water interface.¹⁶ This indicates the possible side effects of large-size PAMAM dendrimers (G5) during the expiration process.

PAMAM Dendrimers Can Efficiently and Safely Cross the DPPC Monolayer during the Expansion Process at Body Temperature. Because the entire breathing process involves both the compression (expiration) and expansion (inhalation) processes, we further investigated the effects of PAMAM dendrimers on DPPC monolayers at the air–water interface during the expansion process at body temperature. Different from the compression process, all PAMAM dendrimers could easily cross the DPPC monolayer without inducing any membrane protrusion of the lipid monolayer (Figure 6a). These interaction differences can be explained by the differences in the gradually increasing area per lipid during the expansion process and the gradually decreasing area per lipid during the compression process.^{16,35} Besides, similar to the compression process, charged PAMAM dendrimers (G3-NH₂, G5-NH₂) have higher membrane penetration ability (Figure 6b). They tend to immerse themselves absolutely in the aqueous phase and directly interact with the lipid phosphate head groups, while charge-neutral PAMAM dendrimers (G3-OH, G5-OH) choose to embed themselves

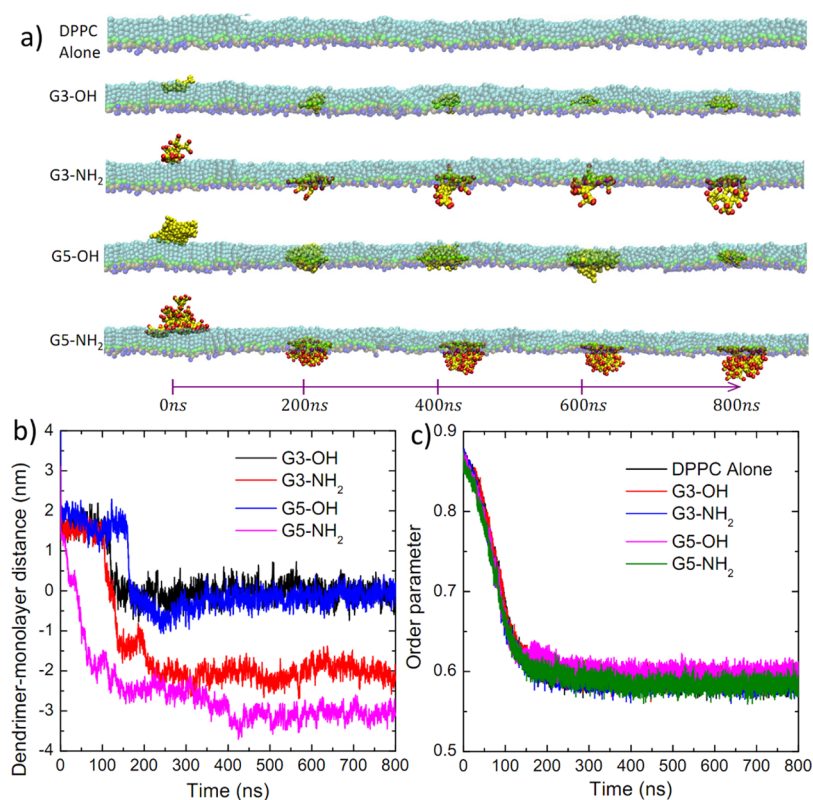


Figure 6. (a) Time-varied changes of system conformations, (b) interfacial lipid chain order parameters, and (c) dendrimer-monolayer distances in the interactions between PAMAM dendrimers and the DPPC monolayer at the air–water interface during the expansion process at $T = 310$ K.

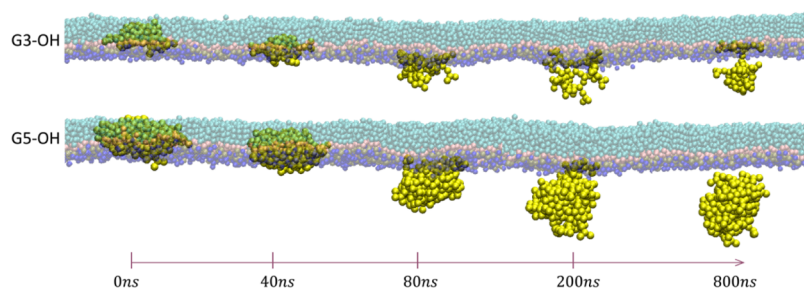


Figure 7. Time-varied conformation changes of system G3-OH and G5-OH during the compression process using the last frame of their expansion simulations as shown in Figure 6a.

in the regions enriching lipid head groups and glycerol groups (Figure 6a,b). In all cases, PAMAM dendrimers show no effects on the normal phase transition of the interfacial lipid acyl chains (Figures 6c and S3). In other words, side effects of large-size PAMAM dendrimers during the compression process could probably be minimized in the subsequent expansion process.

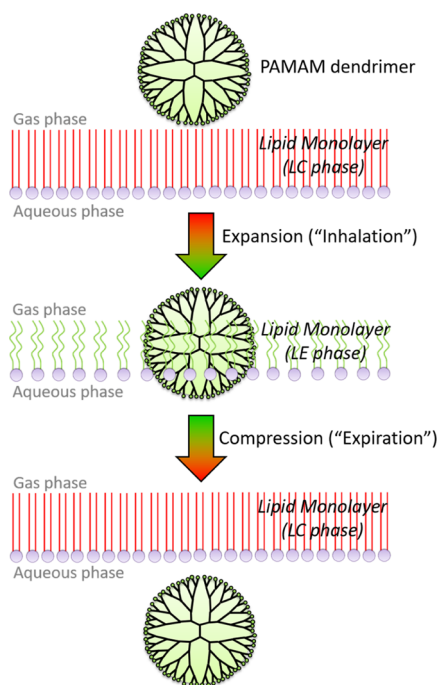
During the expansion (inhalation) process, all PAMAM dendrimers show no obvious effects on both the structure and function of DPPC monolayers. Besides, PAMAM dendrimers almost completely (charged PAMAM dendrimers) and half (neutral PAMAM dendrimers) cross the DPPC monolayer at the air–water interface (Figure 6b). We further probed the possibility that neutral PAMAM dendrimers were squeezed out completely into the aqueous phase without membrane disruptions and the normal phase transition inhibition in the subsequent compression process, which was validated by our simulation results (Figure 7 and Scheme 1). Combining all the interaction information between PAMAM dendrimers and

DPPC monolayers during both the compression and expansion process, we could conclude that adverse effects of large-size PAMAM dendrimers during the compression process might be greatly reduced in the subsequent expansion–compression cycle. In other words, the rapid penetration ability of inhaled PAMAM dendrimers during the inhalation–expiration cycle can greatly reduce their possible side effects during the expiration process, which makes hydrophilic PAMAM dendrimers suitable for respiratory drug carriers.

CONCLUSIONS

In this work, we performed a series of CGMD simulations as well as Langmuir monolayer experiments to probe the possibility of the PAMAM dendrimer as a respiratory drug nanocarrier. We found that the environmental temperature could dramatically affect the interactions of PAMAM dendrimers with the model PS membrane. Hence, experiments and simulations at room temperature could not be directly used to elucidate the interactions between PAMAM

Scheme 1. Schematic for the PAMAM Dendrimer with Higher Penetration Ability and Less Side Effects on the Lipid Monolayer at the Air–Water Interface during an Expansion–Compression Cycle



dendrimers and the model PS membrane at body temperature. CGMD simulations at body temperature found that PAMAM dendrimers could easily cross the model PS membrane during the expansion process, while large-size PAMAM dendrimers might induce adverse effects during the compression process. These adverse effects could be largely minimized and the penetration ability of the PAMAM dendrimers might be dramatically improved in the subsequent respiratory cycle. All these results indicate that hydrophilic and flexible PAMAM dendrimers manifest little effects on the first biological barrier, that is, PS, in respiratory administration, and hence may be used as a respiratory drug nanocarrier.

■ ASSOCIATED CONTENT

📄 Supporting Information

The Supporting Information is available free of charge on the ACS Publications website at DOI: [10.1021/acs.langmuir.9b00434](https://doi.org/10.1021/acs.langmuir.9b00434).

Time-varied changes of system conformations and (b) dendrimer-monolayer distances; phase behaviors of the interfacial DPPC molecules in the interactions of PAMAM dendrimers with the DPPC monolayer at the air–water interface during the expansion process at room temperature; and phase behaviors of the interfacial DPPC molecules in the interactions of PAMAM dendrimers with the DPPC monolayer at the air–water interface during the expansion process at body temperature (PDF)

■ AUTHOR INFORMATION

Corresponding Authors

*E-mail: linxbseu@buaa.edu.cn (X.L.).

*E-mail: yzuo@hawaii.edu (Y.Y.Z.).

*E-mail: guning@seu.edu.cn (N.G.).

ORCID

Xubo Lin: 0000-0002-4417-3582

Yi Y. Zuo: 0000-0002-3992-3238

Ning Gu: 0000-0003-0047-337X

Notes

The authors declare no competing financial interest.

■ ACKNOWLEDGMENTS

The authors thank the anonymous reviewers for the insightful comments. This work was supported by the Fundamental Research Funds for the Central Universities and the Startup Fund of Beijing Advanced Innovation Center for Biomedical Engineering (X.L.), the National Natural Science Foundation of China (nos. 61420106012, 61601227, N.G.), and NSF grants (CBET-1254795 and CBET-1604119, Y.Y.Z.). Computational resources are provided by the Supercomputing Center of Beihang University and Southeast University.

■ REFERENCES

- (1) Wilhelm, S.; Tavares, A. J.; Dai, Q.; Ohta, S.; Audet, J.; Dvorak, H. F.; Chan, W. C. W. Analysis of Nanoparticle Delivery to Tumours. *Nat. Rev. Mater.* **2016**, *1*, 16014.
- (2) Torrice, M. Does Nanomedicine Have a Delivery Problem? *ACS Cent. Sci.* **2016**, *2*, 434–437.
- (3) Gupta, A. K.; Wang, X.; Pagaba, C. V.; Prakash, P.; Sarkar-Banerjee, S.; Putkey, J. A.; Gorfe, A. A. Multi-target, ensemble-based virtual screening yields novel allosteric KRAS inhibitors at high success rate. *Chem. Biol. Drug. Design* **2019**, DOI: [10.1111/cbdd.13519](https://doi.org/10.1111/cbdd.13519).
- (4) Dombu, C.; Carpentier, R.; Betbeder, D. Influence of Surface Charge and Inner Composition of Nanoparticles on Intracellular Delivery of Proteins in Airway Epithelial Cells. *Biomaterials* **2012**, *33*, 9117–9126.
- (5) Yang, M. Y.; Chan, J. G. Y.; Chan, H.-K. Pulmonary Drug Delivery by Powder Aerosols. *J. Controlled Release* **2014**, *193*, 228–240.
- (6) Zhou, Q.; Leung, S. S. Y.; Tang, P.; Parumasivam, T.; Loh, Z. H.; Chan, H.-K. Inhaled Formulations and Pulmonary Drug Delivery Systems for Respiratory Infections. *Adv. Drug Delivery Rev.* **2015**, *85*, 83–99.
- (7) Kono, K. Dendrimer-based Bionanomaterials Produced by Surface Modification, Assembly and Hybrid Formation. *Polym. J.* **2012**, *44*, 531–540.
- (8) Mecke, A.; Majoros, I. J.; Patri, A. K.; Baker, J. R.; Banaszak Holl, M. M.; Orr, B. G. Lipid Bilayer Disruption by Polycationic Polymers: The Roles of Size and Chemical Functional Group. *Langmuir* **2005**, *21*, 10348–10354.
- (9) Leroueil, P. R.; Hong, S.; Mecke, A.; Baker, J. R.; Orr, B. G.; Banaszak Holl, M. M. Nanoparticle Interaction with Biological Membranes: Does Nanotechnology Present a Janus Face? *Acc. Chem. Res.* **2007**, *40*, 335–342.
- (10) Tomalia, D. A. Birth of a New Macromolecular Architecture: Dendrimers as Quantized Building Blocks for Nanoscale Synthetic Polymer Chemistry. *Prog. Polym. Sci.* **2005**, *30*, 294–324.
- (11) Tian, W.-d.; Ma, Y.-q. Theoretical and Computational Studies of Dendrimers as Delivery Vectors. *Chem. Soc. Rev.* **2013**, *42*, 705–727.
- (12) Tian, W.-d.; Ma, Y.-q. Insights into the endosomal escape mechanism via investigation of dendrimer-membrane interactions. *Soft Matter* **2012**, *8*, 6378–6384.
- (13) Kanchi, S.; Suresh, G.; Priyakumar, U. D.; Ayappa, K. G.; Maiti, P. K. Molecular Dynamics Study of the Structure, Flexibility, and Hydrophilicity of PETIM Dendrimers: A Comparison with PAMAM Dendrimers. *J. Phys. Chem. B* **2015**, *119*, 12990–13001.

- (14) Kanchi, S.; Gosika, M.; Ayappa, K. G.; Maiti, P. K. Dendrimer Interactions with Lipid Bilayer: Comparison of Force Field and Effect of Implicit vs Explicit Solvation. *J. Chem. Theory Comput.* **2018**, *14*, 3825–3839.
- (15) Quintana, A.; Raczka, E.; Piehler, L.; Lee, I.; Myc, A.; Majoros, I.; Patri, A. K.; Thomas, T.; Mulé, J.; Baker, J. R., Jr. Design and Function of a Dendrimer-based Therapeutic Nanodevice Targeted to Tumor Cells through the Folate Receptor. *Pharmacol. Res.* **2002**, *19*, 1310–1316.
- (16) Zuo, Y. Y.; Veldhuizen, R. A. W.; Neumann, A. W.; Petersen, N. O.; Possmayer, F. Current perspectives in pulmonary surfactant - Inhibition, enhancement and evaluation. *Biochim. Biophys. Acta, Biomembr.* **2008**, *1778*, 1947–1977.
- (17) Melbourne, J.; Clancy, A.; Seiffert, J.; Skepper, J.; Tetley, T. D.; Shaffer, M. S. P.; Porter, A. An investigation of the carbon nanotube - Lipid interface and its impact upon pulmonary surfactant lipid function. *Biomaterials* **2015**, *55*, 24–32.
- (18) Baoukina, S.; Monticelli, L.; Amrein, M.; Tieleman, D. P. The Molecular Mechanism of Monolayer-bilayer Transformations of Lung Surfactant from Molecular Dynamics Simulations. *Biophys. J.* **2007**, *93*, 3775–3782.
- (19) Sachan, A. K.; Harishchandra, R. K.; Bantz, C.; Maskos, M.; Reichelt, R.; Galla, H.-J. High-Resolution Investigation of Nanoparticle Interaction with a Model Pulmonary Surfactant Monolayer. *ACS Nano* **2012**, *6*, 1677–1687.
- (20) Tatur, S.; Badia, A. Influence of Hydrophobic Alkylated Gold Nanoparticles on the Phase Behavior of Monolayers of DPPC and Clinical Lung Surfactant. *Langmuir* **2012**, *28*, 628–639.
- (21) Dwivedi, M. V.; Harishchandra, R. K.; Koshkina, O.; Maskos, M.; Galla, H.-J. Size Influences the Effect of Hydrophobic Nanoparticles on Lung Surfactant Model Systems. *Biophys. J.* **2014**, *106*, 289–298.
- (22) Casals, C.; Cañadas, O. Role of Lipid Ordered/Disordered Phase Coexistence in Pulmonary Surfactant Function. *Biochim. Biophys. Acta, Biomembr.* **2012**, *1818*, 2550–2562.
- (23) Discher, B. M.; Schief, W. R.; Vogel, V.; Hall, S. B. Phase Separation in Monolayers of Pulmonary Surfactant Phospholipids at the Air-Water Interface: Composition and Structure. *Biophys. J.* **1999**, *77*, 2051–2061.
- (24) Xu, L.; Zuo, Y. Y. Reversible Phase Transitions in the Phospholipid Monolayer. *Langmuir* **2018**, *34*, 8694–8700.
- (25) Keating, E.; Zuo, Y. Y.; Tadayyon, S. M.; Petersen, N. O.; Possmayer, F.; Veldhuizen, R. A. W. A Modified Squeeze-out Mechanism for Generating High Surface Pressures with Pulmonary Surfactant. *Biochim. Biophys. Acta, Biomembr.* **2012**, *1818*, 1225–1234.
- (26) Luo, Z.; Li, S.; Xu, Y.; Yan, Z.; Huang, F.; Yue, T. The Role of Nanoparticle Shape in Translocation across the Pulmonary Surfactant Layer Revealed by Molecular Dynamics Simulations. *Environ. Sci.: Nano* **2018**, *5*, 1921–1932.
- (27) Berényi, S.; Mihály, J.; Wacha, A.; Tóke, O.; Bóta, A. A Mechanistic View of Lipid Membrane Disrupting Effect of PAMAM Dendrimers. *Colloids Surf., B* **2014**, *118*, 164–171.
- (28) Mukherjee, S. P.; Davoren, M.; Byrne, H. J. In vitro mammalian cytotoxicological study of PAMAM dendrimers—Towards quantitative structure activity relationships. *Toxicol. In Vitro* **2010**, *24*, 169–177.
- (29) Tang, P. S.; Mura, M.; Seth, R.; Liu, M. Acute Lung Injury and Cell Death: How Many Ways Can Cells Die? *Am. J. Physiol.* **2008**, *294*, L632–L641.
- (30) Yang, Y.; Xu, L.; Dekkers, S.; Zhang, L. G.; Cassee, F. R.; Zuo, Y. Y. Aggregation State of Metal-Based Nanomaterials at the Pulmonary Surfactant Film Determines Biophysical Inhibition. *Environ. Sci. Technol.* **2018**, *52*, 8920–8929.
- (31) Stachowicz-Kuśnierz, A.; Cwiklik, L.; Korchowicz, J.; Rogalska, E.; Korchowicz, B. The Impact of Lipid Oxidation on the Functioning of a Lung Surfactant Model. *Phys. Chem. Chem. Phys.* **2018**, *20*, 24968–24978.
- (32) Valle, R. P.; Wu, T.; Zuo, Y. Y. Biophysical Influence of Airborne Carbon Nanomaterials on Natural Pulmonary Surfactant. *ACS Nano* **2015**, *9*, 5413–5421.
- (33) Baoukina, S.; Tieleman, D. P. Computer Simulations of Lung Surfactant. *Biochim. Biophys. Acta, Biomembr.* **2016**, *1858*, 2431–2440.
- (34) Lin, X.; Li, Y.; Gu, N. Molecular Dynamics Simulations of the Interactions of Charge-neutral PAMAM Dendrimers with Pulmonary Surfactant. *Soft Matter* **2011**, *7*, 3882–3888.
- (35) Lin, X.; Bai, T.; Zuo, Y. Y.; Gu, N. Promote Potential Applications of Nanoparticles as Respiratory Drug Carrier: Insights from Molecular Dynamics Simulations. *Nanoscale* **2014**, *6*, 2759–2767.
- (36) Luo, Z.; Li, S.; Xu, Y.; Ren, H.; Zhang, X.; Hu, G.; Huang, F.; Yue, T. Extracting Pulmonary Surfactants to Form Inverse Micelles on Suspended Graphene Nanosheets. *Environ. Sci.: Nano* **2018**, *5*, 130–140.
- (37) Baoukina, S.; Monticelli, L.; Risselada, H. J.; Marrink, S. J.; Tieleman, D. P. The Molecular Mechanism of Lipid Monolayer Collapse. *Proc. Natl. Acad. Sci. U.S.A.* **2008**, *105*, 10803–10808.
- (38) Lin, X.; Zuo, Y. Y.; Gu, N. Shape Affects the Interactions of Nanoparticles with Pulmonary Surfactant. *Sci. China Mater.* **2015**, *58*, 28–37.
- (39) Xu, Y.; Deng, L.; Ren, H.; Zhang, X.; Huang, F.; Yue, T. Transport of Nanoparticles across Pulmonary Surfactant Monolayer: A Molecular Dynamics Study. *Phys. Chem. Chem. Phys.* **2017**, *19*, 17568–17576.
- (40) Hess, B.; Kutzner, C.; van der Spoel, D.; Lindahl, E. GROMACS 4: Algorithms for Highly Efficient, Load-Balanced, and Scalable Molecular Simulation. *J. Chem. Theory Comput.* **2008**, *4*, 435–447.
- (41) Marrink, S. J.; Risselada, H. J.; Yefimov, S.; Tieleman, D. P.; de Vries, A. H. The MARTINI Force Field: Coarse Grained Model for Biomolecular Simulations. *J. Phys. Chem. B* **2007**, *111*, 7812–7824.
- (42) Marrink, S. J.; de Vries, A. H.; Mark, A. E. Coarse Grained Model for Semiquantitative Lipid Simulations. *J. Phys. Chem. B* **2004**, *108*, 750–760.
- (43) Lee, H.; Larson, R. G. Molecular Dynamics Simulations of PAMAM dendrimer-induced Pore Formation in DPPC Bilayers with a Coarse-grained Model. *J. Phys. Chem. B* **2006**, *110*, 18204–18211.
- (44) Lee, H.; Larson, R. G. Coarse-Grained Molecular Dynamics Studies of the Concentration and Size Dependence of Fifth- and Seventh-Generation PAMAM Dendrimers on Pore Formation in DMPC Bilayer. *J. Phys. Chem. B* **2008**, *112*, 7778–7784.
- (45) Berendsen, H. J. C.; Postma, J. P. M.; van Gunsteren, W. F.; DiNola, A.; Haak, J. R. Molecular Dynamics with Coupling to an External Bath. *J. Chem. Phys.* **1984**, *81*, 3684–3690.
- (46) Hong, S.; Bielinska, A. U.; Mecke, A.; Keszler, B.; Beals, J. L.; Shi, X.; Balogh, L.; Orr, B. G.; Baker, J. R.; Banaszak Holl, M. M. Interaction of Poly(amidoamine) Dendrimers with Supported Lipid Bilayers and Cells: Hole Formation and the Relation to Transport. *Bioconjugate Chem.* **2004**, *15*, 774–782.